ELSEVIER

International Journal of Mass Spectrometry 185/186/187 (1999) 343–350

International Journal of Mass Spectrometry

Orientational effects in the direct $Cl^- + CH_3Cl$ S_N2 reaction at elevated collision energies: hard-ovoid line-of-centers collision model

Kent M. Ervin

Department of Chemistry and Chemical Physics Program, University of Nevada, Reno, NV 89557, USA

Received 5 June 1998; accepted 27 July 1998

Abstract

The hard-sphere line-of-centers collision model can be extended analytically to include the orientational dependence of both the energy barrier and the critical distance of approach. This hard-ovoid line-of-centers model is applied to the translational activation of the bimolecular nucleophilic substitution (S_N2) reaction, $Cl^- + CH_3Cl \rightarrow ClCH_3 + Cl^-$, for which a direct reaction mechanism was found in recent classical trajectory calculations. The model is compared with recent experiments and the classical trajectory calculations. (Int J Mass Spectrom 185/186/187 (1999) 343–350) © 1999 Elsevier Science B.V.

Keywords: Collision theory; Bimolecular nucleophilic substitution; S_N2 reactions

1. Introduction

Recent guided ion beam experiments [1] and classical trajectory calculations [2] have investigated the collisional activation of the prototype bimolecular nucleophilic substitution (S_N2) reaction,

$$Cl_a^- + CH_3Cl_b \rightarrow Cl_aCH_3 + Cl_b^- \quad (1)$$

This reaction proceeds on a symmetric double-well potential, with a central S_N2 potential energy barrier that is about 11.5 kJ mol^{-1} higher than reactants according to recent ab initio calculations [3]. The experiments show that translational energy is inefficient at promoting reaction (1) [1], consistent with earlier theoretical predictions [4,5]. The experimental cross section [1] rises slowly above an apparent translational energy threshold of 45 ± 15 kJ mol^{-1}, about four times the ab initio potential energy barrier height. Classical trajectory calculations [2] match the threshold energy and the shape of the cross section remarkably well, although the calculated cross sections are more than an order of magnitude higher than experiment. The trajectories show that the reaction proceeds by a *direct* microscopic reaction mechanism, i.e. complex formation due to the ion–dipole well is unimportant at elevated collision energies. At energies just above the apparent threshold, the angular scattering of products in the trajectory calculations is predominantly backward, characteristic of a rebound mechanism, while at higher energies the products become forward scattered, characteristic of a stripping model [2].

Much previous work on reaction (1) and other S_N2

In honor of Professor Michael T. Bowers on the occasion of his 60th birthday.

PII S1387-3806(98)14122-2

reactions has centered on the success or failure of statistical reaction models [6–10]. For the collisionally activated, direct reaction mechanism, statistical models are clearly inappropriate. It is interesting to examine whether simple kinematic collision models for direct reaction might be capable of reproducing the observed energy dependence of the cross section for reaction (1). The best-known simple collision model is the hard-sphere line-of-centers (LOC) model [11,12], for which the cross section is given by Eq. (2),

$$\sigma(E_T) = 0 \qquad \text{if } E_T \leq \epsilon_0 \tag{2a}$$

$$\sigma(E_T) = \pi d^2 \left(\frac{E_T - \epsilon_0}{E_T}\right) \text{ if } E_T > \epsilon_0 \tag{2b}$$

where E_T is the relative translational energy, d is the hard-sphere diameter (sum of the radii of the two reactants), and ϵ_0 is the threshold energy for reaction. The LOC model specifies that the component of the collision energy along the line-of-centers between the reactant molecules must exceed ϵ_0 at the critical distance of approach, which is fixed at the hard-sphere diameter d.

The hard-sphere LOC model predicts a sharply rising cross section from the threshold, strongly at odds with the experimental results for reaction (1). The experimental data were fit with a widely used empirical threshold power law model given by Eq. (3),

$$\sigma(E_T) = \sigma_0 \frac{(E_T - E_0)^N}{E_T} \tag{3}$$

where σ_0, N, and the threshold energy E_0 are adjustable parameters [13]. Eq. (3) is equivalent to the hard-sphere LOC model for $N = 1$ and $\sigma_0 = \pi d^2$. The optimized parameters [1] for reaction (1) were $\sigma_0 = 0.024$ Å^2/eV^{N-1}, $N = 2.64$, and $E_0 = 45 \pm 15$ kJ mol^{-1}. Despite this high threshold energy compared with the ab initio potential barrier height of 11.5 kJ mol^{-1}, the reaction was shown to proceed by conventional backside S_N2 attack at the carbon atom, at least up to 200 kJ mol^{-1} [1].

One possible reason for the failure of the hard-sphere LOC model for reaction (1) is the orientational dependence of both the minimum energy and distance of closest approach. The potential energy surface for reaction (1) is strongly dependent on the orientation of CH_3Cl. Passage over the S_N2 barrier at the minimum energy can only occur if Cl^- approaches the carbon atom exactly along the C–Cl axis of CH_3Cl. For other angles, the barrier height increases and the position of the barrier (the distance of Cl^- from CH_3Cl at the top of the barrier) changes. Modifications to the hard-sphere line-of-centers model to include an orientational dependence of the critical energy and distance have been presented previously [12,14–18]. In this work, the model is applied to the case of a collision between an atom and a molecule with simple functional forms for the orientational dependence that lead to analytical expressions for the cross sections as a function of energy. This model is then applied to reaction (1) and the results compared with the cross sections from experiment [1] and the classical trajectory calculations [2].

2. Collision model

2.1. General orientation-dependent line-of-centers model

In the generalized collision model for an atom–molecule reaction, the total reaction cross section is obtained by integrating the energy- and orientation-dependent reaction opacity function, $P(E_T, b, \gamma, \phi)$, over random initial values of the impact parameter b and the orientation γ and ϕ, according to Eq. (4),

$$\sigma(E_T) = \left(\frac{1}{4\pi}\right) \int_0^{2\pi} \int_0^{\pi} \int_0^{\infty} P(E_T, b, \gamma, \phi) \times 2\pi b \, db \sin\gamma \, d\gamma \, d\phi \tag{4}$$

where γ gives the orientation of the target molecule in the plane of the collision and ϕ is its azimuthal angle of orientation. The angles are defined by a vector indicating the orientation of the reactant molecule relative to the line-of-centers connecting the atom with the center-of-mass of the molecule at the mo-

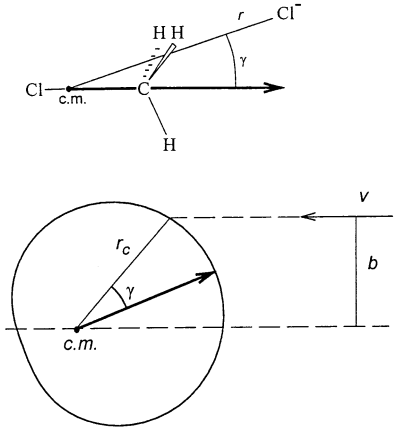

Fig. 1. Geometry parameters used in the hard-ovoid line-of-centers collision model: b, impact parameter; v, relative velocity vector; r_c, critical distance of approach along the line-of-centers; γ, in-plane angle of orientation of the target molecule (bold arrows) relative to the line-of-centers; c.m., center of mass of the target molecule. The curve represents the cross section of the hard-ovoid critical reaction surface, Eq. (12), with $\rho_0 = 4.06$ and $\rho_1 = -1.31$.

ment of reaching a critical minimum separation, $r_c(\gamma, \phi)$. These parameters are shown in Fig. 1. In the line-of-centers model [11,12,14,15], reaction is assumed to occur if the component of the relative kinetic energy along the line-of-centers, E_{LOC}, exceeds a minimum value, $E_0(\gamma, \phi)$. The energy along the line of centers is given by Eq. (5)

$$E_{\mathrm{LOC}} = E_T\left(1 - \frac{b^2}{r_c(\gamma, \phi)^2}\right) \tag{5}$$

Using the line-of-centers criterion, the opacity function is defined by Eq. (6),

$$\begin{aligned} P(E_T, b, \gamma, \phi) &= H(E_{\mathrm{LOC}} - E_0(\gamma, \phi)) \\ &= H[E_T - E_T b^2/r_c(\gamma, \phi)^2 \\ &\quad - E_0(\gamma, \phi)] \end{aligned}$$

where $H(x)$ is the unit step function, i.e. $H(x) = 1$ for $x > 0$ and $H(x) = 0$ for $x \leq 0$. To evaluate the cross section, one must define the functions $r_c(\gamma, \phi)$ and $E_0(\gamma, \phi)$ and integrate Eq. (4) over Eq. (6), setting the integration limits to exclude regions where the opacity function is zero. The integration over impact parameter can be carried out by observing that reaction can occur from $b = 0$ up to a maximum impact parameter $b_{\max}$ in Eq. (7) given by $E_{\mathrm{LOC}} \geq E_0(\gamma, \phi)$,

$$b_{\max}(\gamma, \phi) = r_c(\gamma, \phi)\left(\frac{E_T - E_0(\gamma, \phi)}{E_T}\right)^{1/2} \tag{7}$$

which yields Eq. (8)

$$\begin{aligned} \sigma(E_T) = \frac{1}{4}\int_0^{2\pi}\int_0^{\pi} & r_c(\gamma, \phi)^2 \\ & \times \left(\frac{E_T - E_0(\gamma, \phi)}{E_T}\right) \\ & \times H[E_T - E_0(\gamma, \phi)] \sin\gamma \, d\gamma \, d\phi \end{aligned} \tag{8}$$

For the simple hard-sphere line-of-centers model, both the energy barrier and the critical distance are constants. Integrating Eq. (8) with $r_c(\gamma, \phi) = d$ and $E_0(\gamma, \phi) = \epsilon_0$ gives the well-known result, Eq. (2).

2.2. Orientation-dependent energy barrier

Smith [14] and Levine and Bernstein [15] have previously derived the extension to the line-of-centers model when the energy barrier is dependent on the orientation angle γ. They expand $E_0(\gamma, \phi)$ to first order in $(1 - \cos\gamma)$ according to Eq. (9),

$$E_0(\gamma, \phi) = \epsilon_0 + \epsilon_1(1 - \cos\gamma) \qquad 0 \leq \gamma \leq \pi \tag{9}$$

where ϵ_1 is a positive coefficient, which defines $\gamma = 0$ as the most favorable angle of attack for the case where reaction occurs preferentially at one end of the molecule. The maximum angle $\gamma_{\max}$ given by Eq. (10) defines the cone of acceptance for the reaction

$$\gamma_{\max} = \min\left[\pi, \cos^{-1}\left(\frac{\epsilon_0 + \epsilon_1 - E_T}{\epsilon_1}\right)\right] \tag{10}$$

The integration of Eq. (8) over γ is carried out from limits $\gamma = 0$ to $\gamma_{\max}$ yielding the reaction cross section given by Eqs. (2a), (11a), and (11b)

$$\sigma(E_T) = \pi d^2 \frac{(E_T - \epsilon_0)^2}{4\epsilon_1 E_T} \text{ if } \epsilon_0 < E_T \leq \epsilon_0 + 2\epsilon_1 \tag{11a}$$

$$\sigma(E_T) = \pi d^2\left(\frac{E_T - \epsilon_0 - \epsilon_1}{E_T}\right) \text{ if } E_T > \epsilon_0 + 2\epsilon_1 \tag{11b}$$

Eq. (11) is equivalent to those presented previously [14,15]. Addition of the orientation-dependent energy barrier yields a cross section that is quadratic with the excess energy, smaller in magnitude and less steeply rising than the simple line-of-centers model. At energies above the barrier for all angles of attack, Eq. (11b), the cross section has the same form as the simple line-of-centers model, but with an apparent threshold energy of $\epsilon_0 + \epsilon_1$, equal to the angle-averaged barrier height. Eq. (11b) explicitly limits the maximum cross section to $\sigma = \pi d^2$.

2.3. Orientation-dependent critical distance

In general, the minimum distance of approach as well as the energy barrier varies with orientation. This effect has been included in the angle-dependent LOC framework using ellipsoidal surfaces to define the critical distance [16–18]. For the present S_N2 reaction, where reaction occurs at only one end of the molecule, an appropriate functional form for the orientational dependence of the critical distance is given by Eq. (12),

$$r_c(\gamma) = \rho_0 + \rho_1(1 - \cos\gamma) \qquad 0 \le \gamma \le \pi \tag{12}$$

which represents a curve called a limaçon of Pascal (more generally, $r = a + b\cos\gamma$). Its surface of revolution about the $\gamma = 0$ axis is an ovoid (egg-shaped spheroid). The integration of Eq. (8) using the orientation dependence of the barrier height in Eq. (9) and of the barrier position in Eq. (12) yields analytical expressions for the cross section as a function of collision energy, Eqs. (2a), (13a), and (13b)

$$\sigma(E_T) = \frac{\pi\rho_0^2(E_T - \epsilon_0)^2}{4\epsilon_1 E_T} + \frac{\pi\rho_0\rho_1(E_T - \epsilon_0)^3}{6\epsilon_1^2 E_T} + \frac{\pi\rho_1^2(E_T - \epsilon_0)^4}{24\epsilon_1^3 E_T} \text{ if } \epsilon_0 < E_T \le \epsilon_0 + 2\epsilon_1 \tag{13a}$$

$$\sigma(E_T) = \frac{\pi}{E_T}\left[\rho_0^2(E_T - \epsilon_0 - \epsilon_1) + 2\rho_0\rho_1\left(E_T - \epsilon_0 - \frac{4}{3}\epsilon_1\right) + 2\rho_1^2\left(\frac{2(E_T - \epsilon_0)}{3} - \epsilon_1\right)\right] \text{ if } E_T > \epsilon_0 + 2\epsilon_1 \tag{13b}$$

Inclusion of the orientation-dependent critical distance results in a significantly more complex cross section function. Near threshold, the cross section is a sum of terms of $(E_T - \epsilon_0)^N/E_T$ with powers of $N = 2$, 3, and 4. Because ρ_1 can be positive or negative, the cross section can deviate in either direction from Eq. (11).

If the linear dependence of E_0 and r_c on $(1 - \cos\gamma)$ is not realistic, then higher terms could be added, or the integration could be carried numerically using arbitrary functions of $r_c(\gamma, \phi)$ and $E_0(\gamma, \phi)$. A higher level of complexity involves adding a dependence on ϕ, i.e. a torsional potential. In that case, the integration limits depend on both γ and ϕ. Near threshold, the barrier height might be represented by Eq. (14)

$$E_0(\gamma, \phi) = \epsilon_0 + \epsilon_1(1 - \cos\gamma) + \epsilon_2(1 - \cos\gamma)(1 - \cos n\phi) \tag{14}$$

For the case with $r_c(\gamma, \phi) = d$, one obtains Eq. (15)

$$\sigma(E_T) = \frac{\pi d^2(E_T - \epsilon_0)^2}{4E_T(\epsilon_1^2 + 2\epsilon_1\epsilon_2)^{1/2}} \quad \text{if } \epsilon_0 < E_T \le \epsilon_0 + 2\epsilon_1 \tag{15}$$

near threshold irrespective of n. Thus, the presence of the torsional potential simply reduces the magnitude of the cross section relative to Eq. (11a). For higher energy ranges, or when the critical distance is also orientation dependent, the integration is best done numerically.

3. Application to the $Cl^- + CH_3Cl$ S_N2 reaction

Reaction (1) has a preferred orientation of attack with the chloride atom approaching at the carbon

atom opposite the leaving chloride atom. Treating the orientation as fixed during the direct reaction is crude but reasonable because the mean rotational period for CH_3Cl at room temperature, $\tau_{rot} \approx 2 \times 10^{-12}$ s, is long compared with collision time at the translational energies of the experiments; for example, $\tau_{coll} \approx (1–2) \times 10^{-13}$ s for an interaction distance of 5 Å at relative translational energies of 50–200 kJ mol^{-1}. The LOC collision model neglects effects of the long-range interactions between the reagents as they approach the critical dividing surface. That is most valid for high collision energies, relative to the ion–dipole well depth of 43.5 kJ mol^{-1} for $Cl^- + CH_3Cl$ [19]. The classical trajectory calculations confirm that the reaction proceeds directly without formation of an ion–dipole complex [2]. As discussed previously, statistical models that would be valid for a mechanism involving a complex with randomized internal energy distributions are incapable of reproducing the observed reaction cross section or kinetic isotope effect while also using the accepted barrier height [1].

3.1. Parameters from calculated potential energy surface

Ab initio calculations can be used to estimate the parameters ϵ_0, ϵ_1, ρ_0, and ρ_1. The HF/6-31G* level [20] of theory gives a barrier height for the reaction of 14.9 kJ mol^{-1}, which is slightly too high, and should give qualitatively correct angular dependence. The minimum distance of approach required for reaction is taken as the top of the barrier for S_N2 attack, which is the Cl–CH_3–Cl geometry for a given Cl–C–Cl angle with two identical C–Cl bond distances, and the positions of the hydrogen atoms relaxed. The origin for determining the angle of attack γ and the critical distance r_c is taken as the center-of-mass along the Cl–C axis in chloromethane, i.e. treating CH_3Cl as a pseudo-diatomic. Fig. 2 presents the height of the barrier and the critical distance as a function of $(1 - \cos\gamma)$ for the favorable and unfavorable azimuthal angles ($\phi = 0$ and $\phi = \pi/3$, respectively). The parameters obtained by linear regression fits of Eqs. (9) and (12) to the calculated Hartree–Fock values of E_0 and r_c up to energies of 100 kJ mol^{-1} are given in Table 1. The ab initio values show some curvature, but the linear fits give a reasonable orientation dependence near threshold. The dependence on the azimuthal angle ϕ is not large and will not be considered further, although the dependence would likely be much greater if the hydrogen atom positions were not relaxed in the Hartree–Fock geometry optimizations.

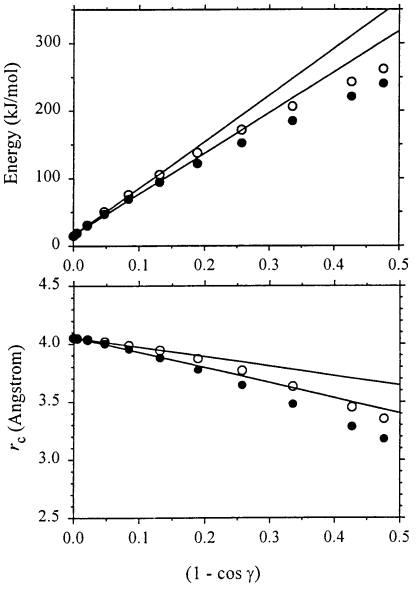

Fig. 2. Orientation dependence of the energy barrier (top) and critical distance (bottom) from the HF/6-31G* potential energy surface, using the center-of-mass of the Cl–CH_3 pseudo-diatomic as the origin. The solid circles give the calculated points for the most favorable torsional angles (e.g. $\phi = 0$) and the open circles are for the unfavorable torsional angles (e.g. $\phi = \pi/3$). The lines are the fits to Eqs. (9) and (12) for near-threshold energies (below 100 kJ mol^{-1}), with parameters listed in Table 1.

Table 1
Model parameters

Parameter	Fit to HF/6-31G* barriers [a]		Fit to experiment
	$\phi = 0$	$\phi = \pi/3$	
ϵ_0 (kJ mol^{-1})	16.5	16.0	11.5 [b]
ϵ_1 (kJ mol^{-1})	603	691	603 [b]
ρ_0 (Å)	4.06	4.05	0.090
ρ_1 (Å)	−1.31	−0.82	3.32

[a] Values obtained for ab initio HF/6-31G* S_N2 barriers as a function of orientation. See text.

[b] Constrained to theoretical values, as described in text.

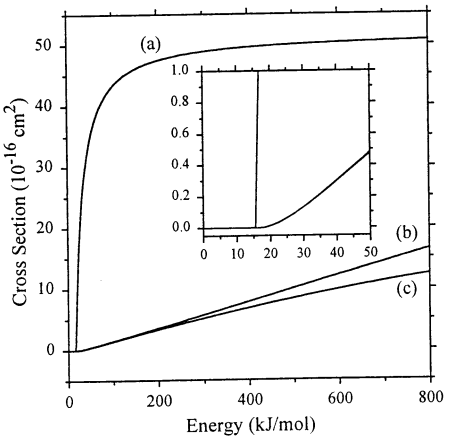

Fig. 3. Calculated model cross sections using the parameters obtained from the HF/6-31G* ab initio calculations. (a) Hard-sphere line-of-centers model, Eq. (2). (b) Hard-sphere line-of-centers model with orientational dependence of the energy barrier, Eq. (11). (c) Hard-ovoid line-of-centers model, with orientational dependence of both the energy barrier and the critical distance, Eq. (13). The inset shows the threshold region magnified.

Fig. 3 shows cross sections calculated using the simple hard-sphere line-of-centers model, Eq. (2); the hard-sphere orientation-dependent-barrier line-of-centers model, Eq. (11); and the hard-ovoid orientation-dependent-barrier line-of-centers model, Eq. (13). Parameters based on the Hartree–Fock values for reaction (1) are used. All three models greatly overestimate the magnitude of the experimental cross section. The behavior of the hard-ovoid model is closer to the experiments than the simple hard-sphere LOC model. In particular, it shows a delayed onset above the threshold. However, the hard-ovoid model still rises too rapidly from the threshold energy compared with experiment.

If the reaction is completely impulsive and the Cl in chloromethane acts as a spectator atom, then using the carbon atom as the origin instead of the center-of-mass of CH_3Cl might better represent the direct dynamics. The calculated energy and especially the critical distance parameters are substantially different for that case, but the features of the calculated hard-ovoid cross sections are qualitatively similar as with the center-of-mass origin. The values of ρ_0 and ρ_1 are smaller, but the cross sections are still larger than experiment.

Both experiment [1] and the classical trajectory calculations [2] show a secondary kinetic isotope effect; the cross section for reaction (1) with CH_3Cl is 16–20% higher than with CD_3Cl. The only mass effect in the hard-ovoid model arises from the shift of center-of-mass origin. However, that results in a negligible difference in the calculated cross sections. Thus, the hard-ovoid model cannot account for the observed kinetic isotope effect. It is possible that consideration of kinetic mass effects [21–23] in the collision could account for the isotope effect, but that is beyond the scope of this article.

3.2. Adjustable-parameter fits

It is quite possible that the model parameters obtained from fits to the Hartree–Fock potential barriers are inadequate, either because the partially relaxed top-of-the barrier geometries picked as the position of the critical distance are unrealistic or because the functional forms for $E_0(\gamma, \phi)$ and $r_c(\gamma, \phi)$ are too simplistic. Therefore, I have also fit the data using ϵ_0, ϵ_1, ρ_0, and ρ_1 as adjustable parameters. Using a full four-parameter fit, a minimum energy barrier of $\epsilon_0 \approx 42$–49 kJ mol^{-1} is obtained. Statistically significant independent values of ϵ_1 and ρ_1 cannot be obtained; that is, the higher terms in Eq. (13a) are not required to fit the data. The energy barrier is similar to the apparent threshold energy of 45 ± 15 kJ mol^{-1} that we obtained using the empirical threshold power law, Eq. (3), where N was treated as an adjustable power [1]. Thus, as a completely empirical function, Eq. (13) has little advantage over Eq. (3).

It is interesting to establish whether the hard-ovoid model can reproduce the experimental results with the threshold energy constrained to the ab initio barrier height. The fit using $\epsilon_0 = 11.5$ kJ mol fixed from G2(+) calculations [3] and $\epsilon_1 = 603$ kJ mol^{-1} based on the Hartree–Fock calculations, and then optimizing the two distance parameters (Table 1) is shown in Fig. 4. Although the quality of this fit is not as good as a four-parameter fit, it is noteworthy that it is possible to reproduce the general cross section behavior near threshold with the hard-ovoid model using the ab initio barrier height. That suggests that orientational

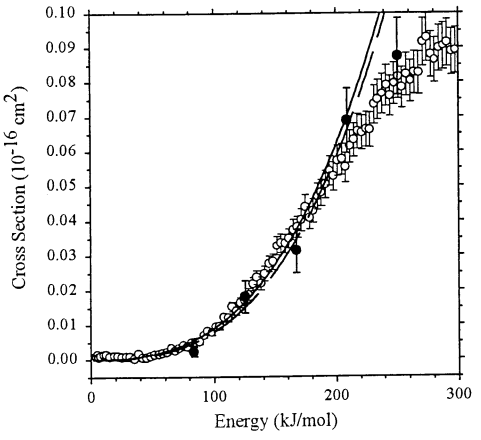

Fig. 4. Fit of Eq. (13) to the experimental data for reaction (1) using a fixed value of ϵ_0 = 11.5 kJ mol^{-1} based on the ab initio barrier height. Other parameters are given in the last column of Table 1. The values of ρ_0 and ρ_1 are optimized over the range 0–200 kJ mol^{-1}. The dashed line is Eq. (13) using the optimized parameters; the solid line is convoluted over experimental energy distributions. The open circles are experimental cross sections [1]. The solid circles are from classical trajectory calculations [2], reduced by a factor of 12 to match the experimental results.

restrictions can partially explain the experimental behavior. However, the required critical distances are much too short to be physically reasonable ($r_c = \rho_0 = 0.09$ Å at $\gamma = 0°$), which implies that the reaction probability is reduced for reasons other than merely orientational effects. For example, there may be collisions where the reactants reach the critical distance of approach, but then rebound. That is the equivalent of recrossings of the dividing surface in transition state theory [14], which have been shown to be prevalent for reaction (1) in classical trajectory calculations at thermal energies [24,25].

For comparison, I also show in Fig. 4 the results of the classical trajectory calculations [2] for the translationally activated reaction, reduced by a factor of 12 to match the experimental magnitudes. The shape of the cross sections are similar, which is encouraging. It would be interesting to investigate the classical trajectories further to determine whether the orientational dependence predicted by the hard-ovoid model is reasonable, and whether a critical distance of approach can be defined that separates reactive and nonreactive trajectories.

4. Conclusion

Orientational effects dramatically alter the threshold behavior of the collision cross section model from the simple hard-sphere line-of-centers model. With an orientation-dependent energy barrier, the cross section rises much more slowly above the threshold energy than predicted by the hard-sphere LOC model. The effects of including the dependence of the critical distance on orientation and the azimuthal anglular dependence are less dramatic. The derived functional form of the hard-ovoid LOC model cross section, Eq. (13a), provides further justification for the use of the empirical threshold law, Eq. (3), near threshold.

For the S_N2 reaction of Cl^- with CH_3Cl, the hard-ovoid line-of-centers collision model can partly explain the experimental results. Although the model can reproduce the general shape of the experimental and classical trajectory cross sections, using model parameters obtained directly from ab initio calculations yields unreasonably high cross section magnitudes. It is not surprising that a collision theory model does not completely explain the S_N2 reaction dynamics. Nevertheless, the hard-ovoid model shows that orientational effects can push the threshold onset of the reaction cross section to energies significantly higher than the minimum potential barrier, as is observed experimentally.

Acknowledgements

This work was supported by the U.S. Department of Energy, Basic Energy Sciences Program. I thank David Mann and Bill Hase for providing numerical values from their classical trajectory calculations.

References

[1] V.F. DeTuri, P.A. Hintz, K.M. Ervin, J. Phys. Chem. A 101 (1997) 5969; see also references therein.
[2] D.J. Mann, W.L. Hase, J. Phys. Chem. A, 102 (1998) 6208.
[3] M.N. Glukhovtsev, A. Pross, L. Radom, J. Am. Chem. Soc. 117 (1995) 2024.

[4] S.R. Vande Linde, W.L. Hase, J. Am. Chem. Soc. 111 (1989) 2349.
[5] S.R. Vande Linde, W.L. Hase, J. Chem. Phys. 93 (1990) 7962.
[6] S.T. Graul, M.T. Bowers, J. Am. Chem. Soc. 113 (1991) 9696.
[7] A.A. Viggiano, R.A. Morris, J.S. Paschkewitz, J.F. Paulson, J. Am. Chem. Soc. 114 (1992) 10477.
[8] S.T. Graul, M.T. Bowers, J. Am. Chem. Soc. 116 (1994) 3875.
[9] W.L. Hase, Science 266 (1994) 998.
[10] S.L. Craig, J.I. Brauman, Science 276 (1997) 1536.
[11] I.W.M. Smith, Kinetics and Dynamics of Elementary Gas Reactions, Butterworths, London, 1980.
[12] R.D. Levine, R.B. Bernstein, Molecular Reaction Dynamics and Chemical Reactivity, Oxford University Press, New York, 1987.
[13] P.B. Armentrout, in Advances in Gas Phase Ion Chemistry, N.B. Adams, L.M. Babcock (Eds.), JAI Press, Greenwich, CT, 1992, Vol. 1, p. 83.
[14] I.W.M. Smith, J. Chem. Educ. 59 (1982) 9.
[15] R.D. Levine, R.B. Bernstein, Chem. Phys. Lett. 105 (1984) 467.
[16] G.T. Evans, R.S.C. She, R.B. Bernstein, J. Chem. Phys. 82 (1985) 2258.
[17] M.H.M. Janssen, S. Stolte, J. Phys. Chem. 97 (1987) 5480.
[18] J.N.L. Connor, W. Jakubetz, J. Chem. Soc. Faraday Trans. 89 (1993) 1481.
[19] C. Li, P. Ross, J.E. Szulejko, T.B. McMahon, J. Am. Chem. Soc. 118 (1996) 9360.
[20] M.J. Frisch, G.W. Trucks, H.B. Schlegel, P. Gill, B.G. Johnson, M.A. Robb, J.R. Cheeseman, T. Keith, G.A. Petersson, J.A. Montgomery, K. Raghavachari, M.A. Al-Laham, V.G. Zakrzewski, J.V. Ortiz, J.B. Foresman, J. Cioslowski, B.B. Stefanov, A. Nanayakkara, M. Challacombe, C.Y. Peng, P.Y. Ayala, W. Chen, M.W. Wong, J.L. Andres, E.S. Replogle, R. Gomperts, R.L. Martin, D.J. Fox, J.S. Binkley, D.J. Defrees, J. Baker, J.P. Stewart, M. Head-Gordon, C. Gonzalez, J.A. Pople, GAUSSIAN 94; Revision D.4, Pittsburgh, PA, Gaussian, Inc., 1995.
[21] A. Miklavc, M. Perdih, I.W.M. Smith, Chem. Phys. Lett. 241 (1995) 415.
[22] M. Perdih, A. Miklavc, I.W.M. Smith, J. Chem. Phys. 106 (1997) 5478.
[23] M. Perdih, I.W.M. Smith, A. Miklavc, J. Phys. Chem. A 102 (1998) 3907.
[24] S.R. Vande Linde, W.L. Hase, J. Phys. Chem. 94 (1990) 6148.
[25] Y.J. Cho, S.R. Vande Linde, L. Zhu, W.L. Hase, J. Chem. Phys. 96 (1992) 8275.